Article

Seed Fatty Acid Changes Germination Response to Temperature and Water Potentials in Six Sesame (*Sesamum indicum* L.) Cultivars: Estimating the Cardinal Temperatures

Hamidreza Balouchi [1,*], Vida Soltani Khankahdani [1], Ali Moradi [1], Majid Gholamhoseini [2], Ramin Piri [3], Seyedeh Zahra Heydari [1] and Beata Dedicova [4,*]

1. Department of Agronomy and Plant Breeding, Yasouj University, Yasouj 7591874831, Iran; vidasoltani73@gmail.com (V.S.K.); amoradi@yu.ac.ir (A.M.) shdy.hy2000@gmail.com (S.Z.H.)
2. Department of Oilseed Research, Seed and Plant Improvement Institute, Agricultural Research, Education and Extension Organization (AREEO), Karaj 3135933151, Iran; m.gholamhoseini@areeo.ac.ir
3. Department of Agronomy and Plant Breeding, University of Tehran, Tehran 3158777871, Iran; raminpiri88@yahoo.com
4. Department of Plant Breeding, Swedish University of Agricultural Sciences (SLU), P.O. Box 190, 234 22 Lomma, Sweden
* Correspondence: balouchi@yu.ac.ir (H.B.); beata.dedicova@slu.se (B.D.)

Abstract: Seed fatty acid composition can influence seed quality, followed by seed germination and optimal seedling establishment. Therefore, to find out the role of seed fatty acids in changing the cardinal temperatures of six sesame cultivars germinated at different temperatures (10, 15, 20, 25, 30, 35, 40, and 45 °C) and water potentials (0, −0.2, −0.4, −0.6, −0.8, −1, and −1.2 MPa), an experiment was conducted. The dent-like, beta, and segmented models were used to analyze the data. The results showed that different cultivars at optimal temperatures show different reactions to environmental conditions; for example, the germination rate in Halil and Dashtestan2 cultivars followed the dent-like model, Darab1, Oltan, and Yellow-White followed the beta model, and Naz followed the segmented model. Based on the results, the average temperature in all water potentials of the base, sub-optimal, supra-optimum, and ceiling was determined as 12.6, 33.3, 38, and 43.9 °C, respectively, once the superior dent-like model was used. Using the superior beta model, the average temperatures in the base, optimum, and ceiling were 8.5, 31.2, and 50.5 °C. In contrast, when the segmented superior model was used, they were determined to be 7.6, 34, and 44.1 °C, respectively. According to the results, it can be stated that the Halil cultivar with more oleic acid and less linoleic acid has a higher base temperature and is more adapted to high temperatures for later cultivations. The Naz cultivar with a long biological clock is suitable for earlier cultivations. The ceiling temperature of these cultivars was also affected by the osmotic potential and decreased significantly with the increase in osmotic levels. Dashtestan2 cultivar with a high germination rate could be chosen for cultivation in water and high-temperature stress areas.

Keywords: basal temperature; germination modeling; germination rate; seed moisture; seed oil

1. Introduction

Temperature is a limiting factor for plants' metabolism at the cellular level and growth and development at the tissue or organ level. In such a way, the beginning, completion, and amount of plant metabolism are affected by temperature [1]. The maximum germination percentage of plants occurs in a specific temperature range, and germination would be affected by its fluctuation (falling and rising) in this temperature range [2]. Plants have three specific (cardinal) temperatures, including the base or minimum temperature, the optimal temperature, and the maximum or ceiling temperature for germination. The base and maximum temperatures are the temperatures where seed germination would stop

below and above them, while the optimal temperature is the temperature at which the germination can occur in the shortest time; in other words, the germination rate is at its maximum. Moreover, the germination rate increases with increasing temperature up to the optimal germination temperature and decreases after that [3].

In addition to temperature, soil water potential is one of the most critical environmental factors affecting plant germination and establishment [4]. Regarding reducing water potential, studies show that lowering water potential minimizes the chance of plant establishment, uniform greening, germination rate, and yield. Moreover, the ability of seeds to germinate under conditions of different temperatures and water potential increases the chance of plant establishment and higher plant density, which ultimately leads to increased yield [5]. Different temperature and water potential conditions can affect seed germination through changes in seed composition, including seed oil and carbohydrates [6]. It has been reported that *Bidens pilosa* L. (Asteraceae) [7] and maize (*Zea mays* L.) [8] seed populations had different germination responses to temperature and water potential, and the optimal and ceiling temperatures were varied.

Germination is frequently regarded as a crucial stage in the life cycle of plants because of its extreme sensitivity to variables, including water, temperature, light, and gas environment [9]. When access to water is not a problem, the temperature is the primary determinant of germination [10]. Using seed germination models, modeling science can determine critical plant seed temperatures [11]. Using segmented and beta models, base, optimal, and maximum germination temperatures can be estimated. Still, the dent-like model's optimal temperature range is evaluated from the first to the second optimal temperature [12]. In these models, the linear relationship between the germination rate and the increase in temperature from the base temperature to the optimal temperature and the rise in temperature from the optimal temperature to the ceiling temperature is well exhibited. Favorable germination conditions predict the next stage of seedling growth and development [11,13].

Sesame (*Sesamum indicum* L.) is an oilseed crop grown for its edible oil in dry and semi-arid conditions worldwide. Because of its minimal input requirements, it is a great crop to cultivate in rotation with other crops [14]. Sesame seeds are rich in oil, and the seed quality of this plant directly or indirectly depends on the quality of the oil and the composition of fatty acids that make up the structure of the oil [15]. The composition of sesame oil's fatty acids, namely oleic (monounsaturated fatty acid), palmitic (saturated fatty acid), linoleic, and linolenic (polyunsaturated fatty acid) acids [16,17], determines its quality. The relative concentration of these fatty acids is determined mainly by cultivar, climatic conditions, and management approaches, and it is critical in deciding oil quality [18,19].

Oil content and fatty acid compounds are essential characteristics of oilseed crops. A few studies have examined the relationship between seed fatty acid composition and germination characteristics. For example, Bello et al. (2014) [20] reported that in sunflowers, basal temperature has an inverse relationship with linoleic acid content, and genotypes with a high percentage of linoleic acid germinated earlier at low temperatures (lower than 15 °C). In addition, the genotype with more stearic and oleic acid showed a lower temperature requirement for germination than the genotype with more stearic and linoleic acid.

It is likely that the seed germination at different temperatures and water potentials is related to the quality characteristics of the seed, including the composition of fatty acids. In addition, investigating the role of fatty acids on the germination response of sesame seeds can be important in determining the planting date and different ecological conditions. Therefore, the objectives of this research included determining the relationship between seed fatty acids and the cardinal temperatures of six sesame seed cultivars and their germination status in different water potentials.

2. Material and Methods

2.1. Plant Material

Sesame cultivars, including Halil, Darab1, Dashtestan2, Oltan, Yellow-White, and Naz, were obtained from the Seed and Plant Improvement Institute of Karaj, Iran, and are essential in the industry, especially oil production. The characteristics of the cultivars are shown in Table 1, and the initial parts of the seed samples are shown in Table 2.

Table 1. Characteristics of the sesame varieties studied.

Cultivars.	Halil	Darab1	Dashtestan2	Oltan	Yellow-White	Naz
Year of introduction	2013	2009	2006	1999	2006	2001
Branching	Branched	Branched	Branched	Branched	Branched	Single branch
Seed color	Brown	light brown	light brown	dark brown	Light cream	Cream
Production Year	2017–2018	2017–2018	2017–2018	2017–2018	2017–2018	2017–2018

Table 2. Essential characteristics of sesame seeds were tested.

Cultivars	Germination Percentages	Thousand Seed Weight (g)	Seed Moisture Content (%)	Oil Percentages
Halil	99	3.8	6.07	58.25
Darab1	98	3.12	5.15	54.77
Dashtestan2	99	3.44	5.37	65.05
Oltan	98	3.25	4.87	57.54
Yellow-white	99	2.91	5.85	52.66
Naz	99	2.85	5.16	54.09

2.2. Test Specifications

The first part of the experiment was to determine the cardinal temperature of the cultivars germinated at different water potentials, and the second part included oil extraction, quantifying fatty acids in each cultivar, and calculating the relationship between fatty acids and the cardinal temperature.

2.3. Cardinal Temperature

The experiment was conducted in the Seed Technology Laboratory, Faculty of Agriculture, Yasouj University, in a completely randomized design with four replications of 25 seeds for each temperature (as environment). To determine cardinal temperatures, seed germination at different temperatures (10, 15, 20, 25, 30, 35, 40, and 45 °C) and water potentials (0, −0.2, −0.4, −0.6, −0.8, −1, and −1.2 MPa) were investigated using dent-like, beta, and segmented models. The seeds were disinfected, placed in a 1% sodium hypochlorite solution for 60 s, and transferred onto 9 cm diameter Petri dishes with filter paper to maintain moisture. Ten ml of osmotic solution was added to each Petri dish, and 10 mL of distilled water was added for a zero MPa level.

Different levels of water potential were prepared through the publication [21] formula and using polyethylene glycol 6000 (Merck, Schuchardt OHG, Hohenbrunn, Germany). The calculation for Equation (1) is as follows:

$$\Psi S = -(1.8 \times 10^{-2})\, C - (1.8 \times 10^{-4})\, C^2 + (2.67 \times 10^{-4})\, CT + (8.39 \times 10^{-7})\, C^2T \qquad (1)$$

In this equation, the osmotic potential ΨS is osmotic pressure in terms of the bar, C is the concentration of PEG-6000 in g/kg H_2O, and T is the temperature of the culture medium in terms of centigrade.

All germination tests were performed under 12/12 h (light/darkness) conditions using a germinator (SG600 model, Germinator noorsanatferdows Co., Karaj, Iran) with a ± 1 °C fluctuation. Each temperature was applied to six cultivars at the desired potential

by placing Petri dishes in the germinator. Counting germinated seeds was carried out every eight hours, and when calculating the seeds whose roots had grown 2 mm or more, they were considered germinated. The following relationships were used to determine the cardinal germination temperature of six sesame cultivars (Equation (2)):

$$R50 = f(T)Rmax \tag{2}$$

In this relationship, $f(T)$ is a function of temperature, which changes from zero at the base and ceiling temperatures to 1 at the desired temperature. $Rmax$ is the maximum intrinsic germination rate at the desired temperature. Therefore, $1/Rmax$ shows the minimum hours until germination at the optimal temperature, which is the same number of biological hours required for germination, through which the following three functions are evaluated.

1. The dent-like temperature function with the abbreviation (D) is as follows (Equation (3)):

$$
\begin{aligned}
f(T) &= \frac{(T-T_b)}{(T_{o1}-T_b)} \quad if \ \ T_b < T \le T_{o1} \\
f(T) &= \frac{(T_c-T)}{(T_c-T_{o2})} \quad if \ \ T_{o2} < T \le T_c \\
f(T) &= 1 \quad \ if \ \ T_{o1} < T \le T_{o2} \\
f(T) &= 0 \quad if \ \ T \le T_b \ or \ T \ge T_c
\end{aligned}
\tag{3}
$$

2. The segmented function with the abbreviation (S) is as follows (Equation (4)):

$$
\begin{aligned}
f(T) &= \frac{(T-T_b)}{(T_o-T_b)} \quad \ if \ \ T_b < T \le T_o \\
f(T) &= \left[1-\left(\frac{T-T_o}{T_c-T_o}\right)\right] \quad if \ \ T_o \le T < T_c \\
f(T) &= 0 \quad \ \ if \ \ T \le T_b \ or \ T \ge T_c
\end{aligned}
\tag{4}
$$

3. The beta function with the abbreviation (B) is as follows, and α is the shape parameter for the beta function that determines the curvature of the function (Equation (5)):

$$f(T) = \left[\left(\frac{T-T_b}{T_o-T_b} \times \frac{T_c-T}{T_c-T_o}\right)^{\left(\frac{T_c-T_o}{T_o-T_b}\right)}\right]^a \ \ if \ \ T > T_b \ and \ T < T_c$$

$$f(T) = 0 \qquad if \ T \le T_b \ or \ T \le T_c \tag{5}$$

In these relationships, T is the average daily temperature (test temperature), T_b is the base temperature, T_{o1} is the suboptimal temperature, T_{o2} is the supraoptimal temperature, and T_c is the ceiling temperature in °C [22].

Moreover, the following criteria were used to select the best model among the above models (Equation (6)):

a. Root Mean Square Error (*RMSE*)

$$RMSE = \sqrt{\frac{\Sigma(p-o)^2}{n-1}} \tag{6}$$

P and O are the predicted values of the germination rate using the model and the observed value, and n is the number of observations.

b. R^2 (Coefficient of determination) (Equation (7))

$$R^2 = 1 - \frac{SSE}{SSG} \tag{7}$$

where *SSE* and *SSG* are the sums of squared error and a sum of total squared, respectively.

c. Simple linear regression coefficients (*a* and *b*) between predicted values and actual values. Coefficients *a* and *b* indicate the deviation of the regression line from the co-ordinate origin and the deviation of the regression line from the 1:1 line, respectively.
d. Linear correlation coefficient (*r*) between observed and predicted germination days.
e. Concordance correlation coefficient (r_c) (Equation (8))

$$r_c = r \times C_b \tag{8}$$

where *r* is Pearson's correlation coefficient, C_b is the accuracy of the model, r_c is based on the predicted value of the germination rate using the model (*X*), the observed value (*Y*), and *N* (the number of observations), calculated based on the following Equation (9):

$$r_c = \frac{2S_{XY}}{S_x^2 + S_Y^2 + (\overline{X} - \overline{Y})^2} \qquad S_{XY} = \frac{1}{N}\sum_{n=1}^{N}(X_n - \overline{X})(Y_n - \overline{Y})$$
$$S_Y^2 = \frac{1}{N}\sum_{n=1}^{N}(Y_n - \overline{Y})^2 \qquad S_x^2 = \frac{1}{N}\sum_{n=1}^{N}(x_n - \overline{x})^2 \tag{9}$$

The comparison of the estimated parameters of cardinal temperatures between the models was carried out based on their 95% confidence limits.

2.4. Seed Oil Extraction and Measurement of Fatty Acids Profile

According to [23], oil extraction was carried out. The seed samples were cleaned by hand, dried in a 105 °C oven for 48 h, and then processed using a grinding machine. A Soxhlet apparatus (Gerhardt, model 173200, EV, Königswinter, Germany) was used to extract oil using petroleum ether at 40–60 °C for four hours. A rotary flash evaporator removed the solvent under reduced pressure (Heidolph, model Laborota 4000, Schwabach, Germany). Following the procedures Azadmard-Damirchi et al. (2010) [24] described, fatty acid methyl esters (FAMEs) were extracted and produced from the oil samples.

Briefly, a vial containing oil (about 10 mg) was added with 2 mL of 0.01 M NaOH dissolved in methanol, followed by 0.5 mL of hexane, and maintained in a water bath at 60 °C for approximately 10 min. After adding boron trifluoride (20% BF3 in methanol), samples were heated for 10 min in a 60 °C water bath. After cooling the samples under running water, 2 mL of 20% (*w/v*) sodium chloride and 1 mL of hexane were added. The mixture was shaken quickly, and the hexane layer containing FAMEs was centrifuged to remove it.

Gas chromatography was used to analyze FAMEs for a fatty acid profile, according to [25]. A flame ionization detector and a split/splitless injector were coupled with a gas chromatograph. A 50 m × 0.22 mm, 0.25 m film thickness fused-silica capillary column BPX70 (SGE, Austin, TX, USA) was installed in the device. Temperatures were chosen for the injector and detector at 230 and 250 °C, respectively. The oven's temperature started at 158 °C, reached 220 °C (2 °C/min), and remained there for 5 min. At a 3.0 mL/min flow rate, helium and N were utilized as the carrier and make-up gases, respectively—the peak areas expressed as a proportion of the total fatty acids allowed for identifying the FAMEs.

2.5. Statistical Analysis

The iterative optimization method with the PROC NLIN procedure of SAS 9.1 statistical software (SAS Institute Inc., Cary, NC, USA) was used to evaluate the model's parameters. The best model in each cultivar was used according to the priority of the matching correlation coefficient (r_c) due to checking the accuracy and precision of the model compared to other evaluation methods that only contain the model's accuracy. Then, the *RMSE*, R^2 and linear correlation coefficient (*r*) were selected, and Excel 2017 software was used to draw graphs related to the models.

3. Results

The results indicated a different cardinal temperature for each genotype, and the germination process of the genotypes does not follow the same pattern. Table 3 shows that the three models' R^2, *RMSE*, r_c, coefficient *a*, and coefficient b were evaluated for cultivars. The dent-like model for Halil and Dashtestan2 cultivars, the beta model for Darab1, Oltan, and Yellow-White cultivars, and the segmented model for Naz cultivars were selected as the superior models. Figures 1–3 show the fitted models of the predicted germination rate and the data obtained from the observed germination rate at different temperatures and water potentials for all six sesame cultivars, given by the method of dent-like, segmented, and beta models.

Table 3. Described model by Dent-like, Beta, or Segmented functions for the relationship between germination rate with temperature and water potential of sesame cultivars, using accordance coefficient (r_c), root mean square of errors (*RMSE*), coefficient of determination (R^2), regression coefficients (*a* and *b*), and the correlation coefficient (*r*).

Variety (Model)	Water Potential (MPa)	r_c	*RMSE*	R^2	*a*	*b*	r
Halil (Dent-like)	0	0.87	0.0067	0.96	0.0015	0.96 **	0.98
	−0.2		0.0112	0.86	0.0041	0.86 **	0.93
	−0.4		0.0102	0.74	0.0051 *	0.74 **	0.86
	−0.6		0.0032	0.62	0.0025 **	0.61 **	0.78
	−0.8		0.0022	0.54	0.0003	0.55 **	0.73
Darab1 (Beta)	0	0.83	0.0080	0.62	0.0083 **	0.63 **	0.79
	−0.2		0.0032	0.71	0.0038 **	0.68 **	0.84
	−0.4		0.0033	0.68	0.0034 **	0.64 **	0.82
	−0.6		0.0022	0.67	0.0022 *	0.67 **	0.82
	−0.8		0.0002	0.99	0.000007	1.01 **	1
Dashtestan2 (Dent-like)	0	0.88	0.0074	0.94	0.0021	0.94 **	0.97
	−0.2		0.0089	0.86	0.0039	0.84 **	0.93
	−0.4		0.0088	0.59	0.0069 **	0.58 **	0.77
	−0.6		0.0083	0.47	0.0079 **	0.41 **	0.69
	−0.8		0.0024	0.58	0.0011 **	0.55 **	0.76
Oltan (Beta)	0	0.79	0.0029	0.74	0.0039 **	0.72 **	0.86
	−0.2		0.0026	0.24	0.0076 **	0.22 **	0.49
	−0.4		0.0031	0.42	0.0039 **	0.40 **	0.65
	−0.6		0.0004	0.99	0.00002	0.99 **	1
	−0.8		-	-	-	-	-
Yellow-white (Beta)	0	0.73	0.0127	0.73	0.0033	0.83 **	0.86
	−0.2		0.0184	0.43	0.0157 **	0.57 **	0.66
	−0.4		0.0139	0.36	0.0104 **	0.52 **	0.60
	−0.6		0.0027	0.42	0.0033 **	0.40 **	0.65
	−0.8		0.0016	0.72	0.0003	0.72 **	0.85
Naz (Segmented)	0	0.75	0.0065	0.89	0.0039 *	0.86 **	0.94
	−0.2		0.0061	0.80	0.0051 **	0.74 **	0.89
	−0.4		0.0052	0.53	0.0062 **	0.43 **	0.73
	−0.6		0.0022	0.64	0.0017 **	0.59 **	0.80
	−0.8		0.0006	0.12	0.0008 **	0.06	0.34

Note: *, ** in *a* and *b* indicate a significant distance with the origin of coordinates and a 1:1 axis at one and five percent of the error probability.
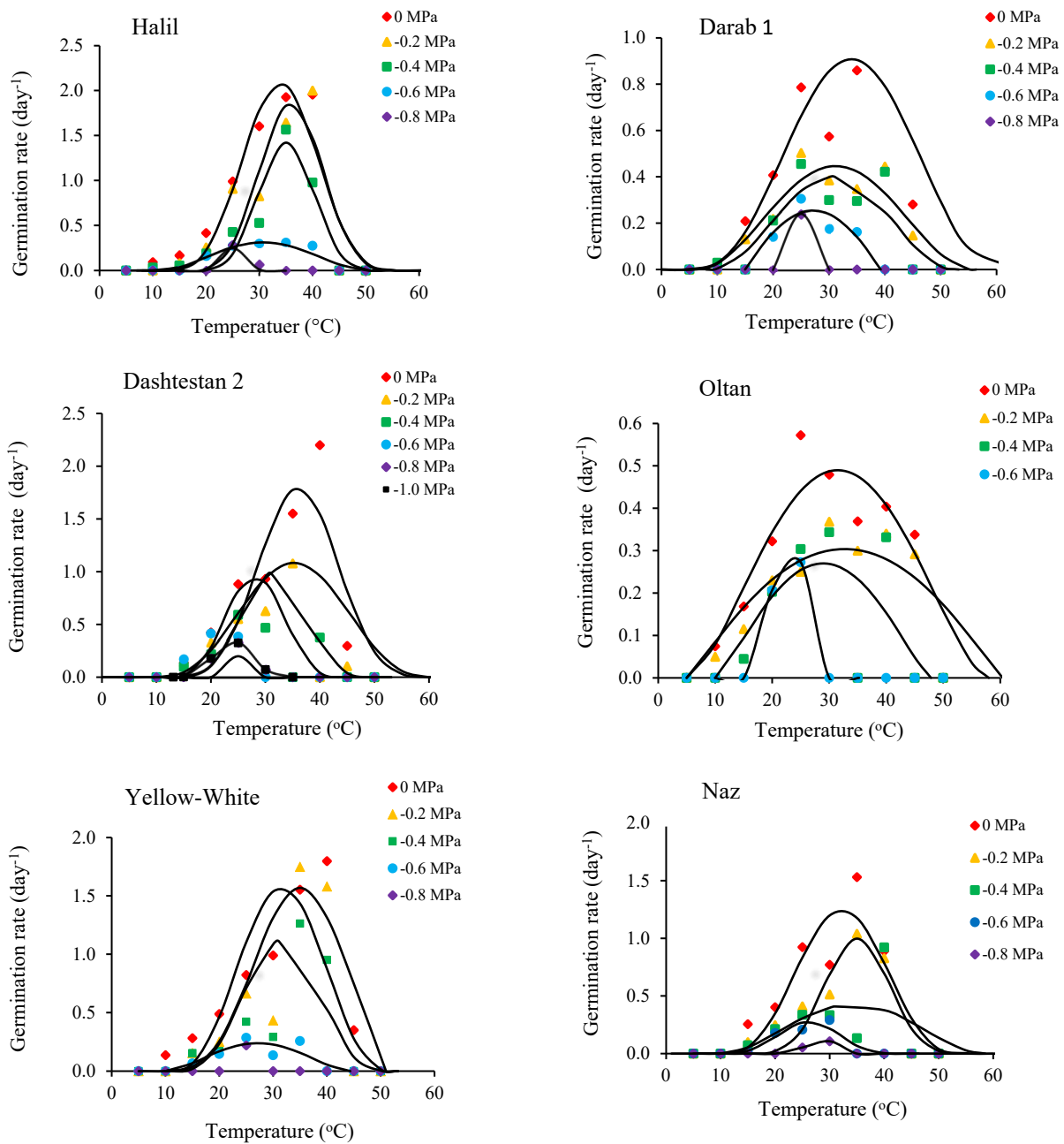
Figure 1. Predicting the germination of sesame cultivars at different temperatures and water potentials using the beta model. The symbols show observed germination, and the lines show expected germination.
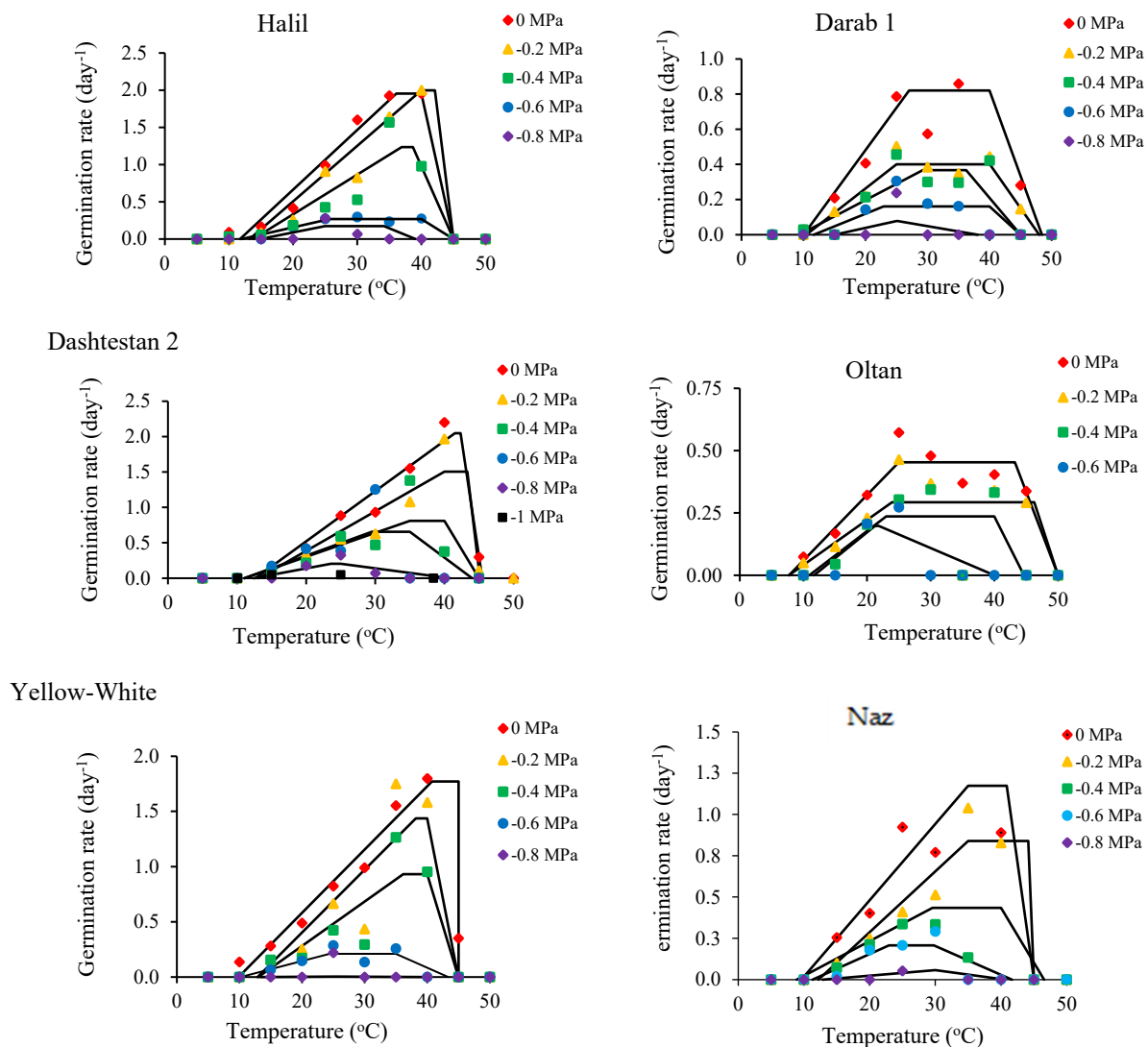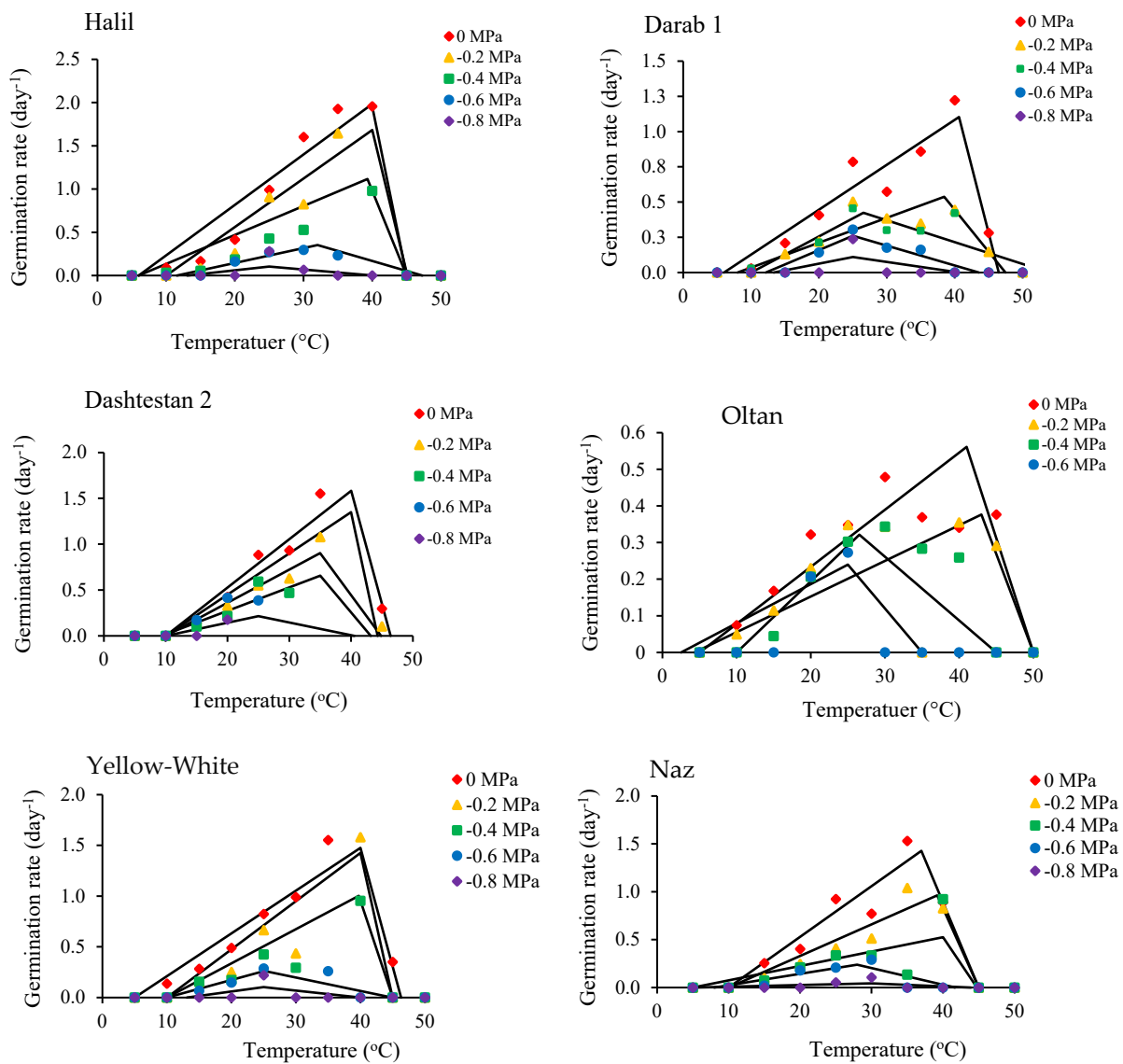
Figure 2. The dent-like model predicts sesame cultivars' germination at different temperatures and water potentials. The symbols show observed germination, and the lines show expected germination.

Figures 1–3 show the fitted models of the predicted germination rate and the data obtained from the observed germination rate at different temperatures and water potentials for all six sesame cultivars, given by the method of dent-like, segmented, and beta models. The superior models with a lower root mean square error and higher R^2 than the other two models were chosen as the best models for these cultivars (Figure 4).

The variations in germination rate among the cultivars under study revealed that, up until the optimum temperature range, germination rate increased with rising temperature and, after that, decreased with an increase in temperature. The highest germination rate was observed at lower temperatures, which shows the adaptation of the plant to drought stress at low temperatures.

The results revealed that the basal temperature varied from 7.5 to 13.1 °C. In all six cultivars, the base temperature was also affected by the amount of fatty acids; therefore, among the cultivars, the cultivar Halil had the highest base temperature (13.1 °C), which can be attributed to the increase in the amount of oleic, palmitic, and arachidic fatty acids and the decrease in linolenic, linoleic, and stearic fatty acids. The lowest base temperature (7.5 °C) was assigned to the Oltan cultivar, which was associated with a decrease in the amount of oleic, palmitic, and arachidic fatty acids and an increase in linolenic, linoleic, and stearic fatty acids (Figure 5).
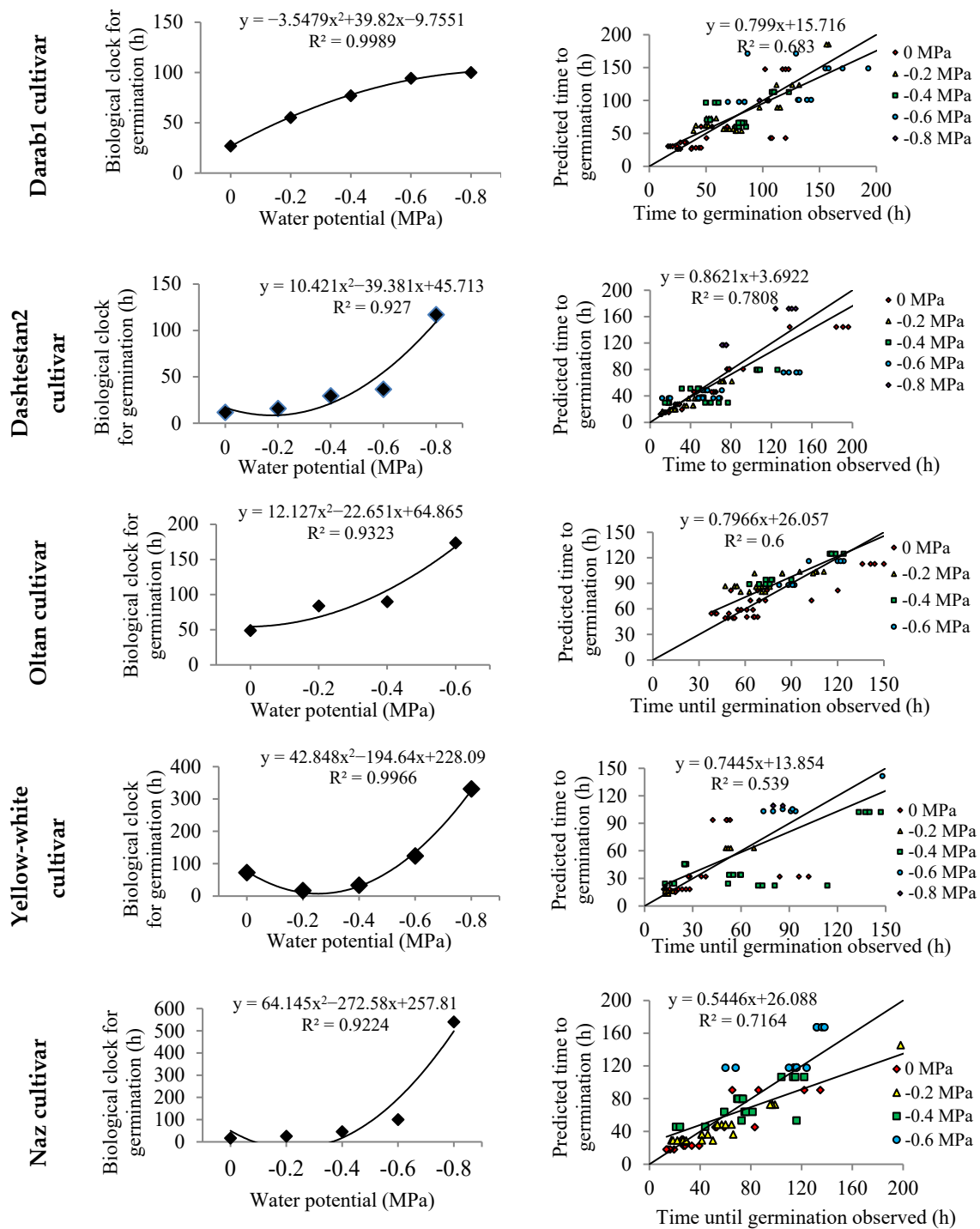
Figure 3. Predicting the germination of sesame cultivars at different temperatures and water potentials using the segmented model. The symbols show observed germination, and the lines show expected germination.
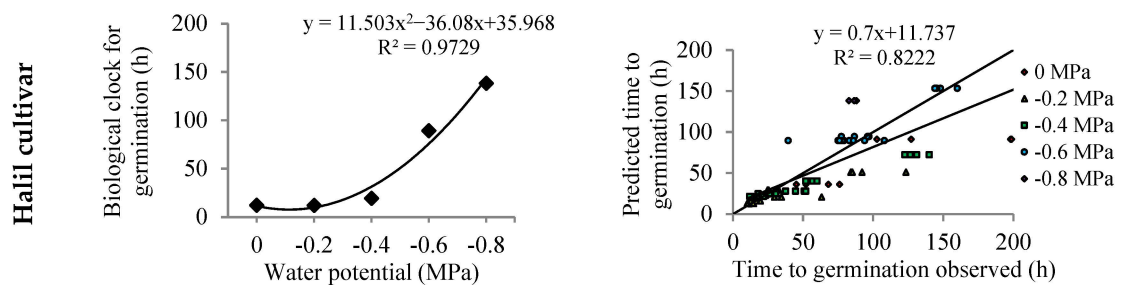
Figure 4. *Cont.*

Figure 4. Changes in biological germination clock and evaluation of models based on comparison of time to predicted germination (h) and observed germination (h) in sesame cultivars at different water potentials (MPa).
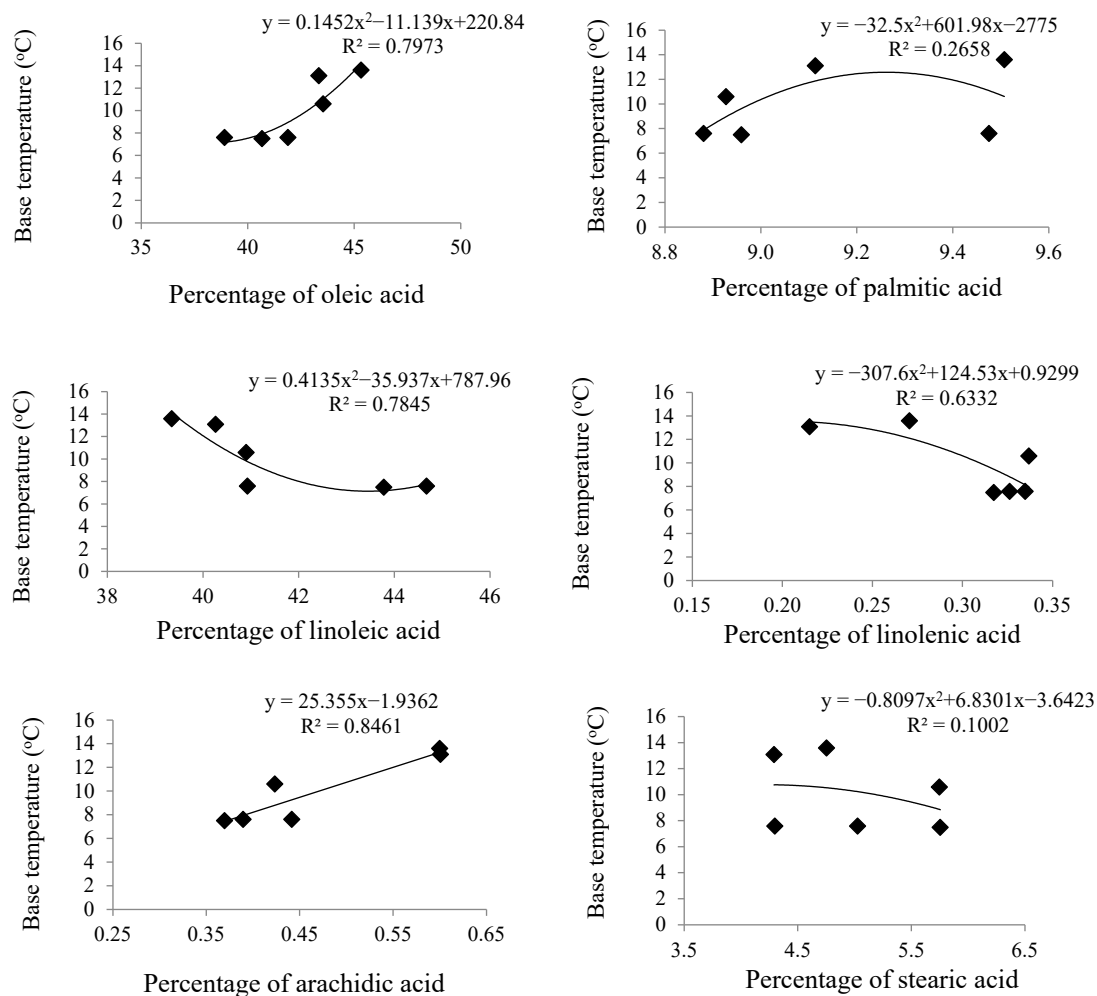
Figure 5. Investigate the relationship between the percentage of fatty acids and the basal temperature of germination in sesame cultivars.

Based on the dent-like model, the optimum temperature (T_{o1}–T_{o2}) for Halil ranged from 32.7 to 38.98 °C and for the Dashtestan2 variety from 33.9 to 37.1 °C (Figures 1–3). The optimum temperature was variable in every six cultivars, and the lowest optimum temperature in the Oltan cultivar was determined to be 27.1 °C. In Halil, Darab1, Dashtestan2, and Oltan cultivars, with the increase in osmotic potential due to drought stress, the base temperature has increased due to the change in the amount of fatty acids in the seeds. In all cultivars, a decrease in the rate and an increase in the biological clock for germination were observed, along with an increase in osmotic potential (Table 4, Figure 4).

In all cultivars (except Oltan), with an increase in osmotic level above −1 MPa, the percentage of germination reached zero, and in this cultivar, with osmotic levels above −0.8 MPa, germination reached zero. At the level of 0 MPa in all cultivars, the highest germination rate (2.04/day) was assigned to the Dashtestan2 cultivar, and the lowest was related to the Yellow-White cultivar with a value of 0.34/day (Table 4). At −0.8 MPa, the highest germination rate (0.24/day) and the highest base temperature (20 °C) were obtained from the Darab1 cultivar.

The ceiling temperature of the cultivars was also affected by the osmotic potential and decreased significantly with the increase in osmotic levels. Moreover, the lowest biological clock for germination was in the Dashtestan2 cultivar, with a value of 42.2 h, and the highest (145.7 h) was related to the Naz cultivar (Table 4).

Table 4. Prediction result of germination cardinal temperatures of Sesame cultivars based on the top model (Dent-like, Beta, or Segmented) at different water potentials.

Cultivar (Top Model)	Water Potential (MPa)	a	T_b (°C)	T_{o1} (°C)	T_{o2} (°C)	T_c (°C)	Rmax (day^{-1})	G_0 (h)
Halil (Dent-like)	0	-	11.7	36.1	40.0	45.0	1.94	12.3
	−0.2	-	13.2	40.0	42.1	45.0	1.99	12.0
	−0.4	-	13.8	36.9	38.7	45.0	1.22	19.4
	−0.6	-	12.0	25.7	40.0	45.0	0.17	89.3
	−0.8	-	14.8	25.0	34.1	39.1	0.17	138.3
Average	-	-	13.1	32.7	39.0	43.8	1.13	54.2
Darab1 (Beta)	0	2.91	4.0	31.8	-	64.0	0.89	26.9
	−0.2	1.87	6.0	28.4	-	56.3	0.43	55.2
	−0.4	1.35	8.0	23.7	-	53.2	0.31	76.9
	−0.6	1.00	14.9	26.6	-	39.3	0.26	94.3
	−0.8	1.00	20.0	25.0	-	30.0	0.24	100.0
Average	-	-	10.6	27.1	-	48.6	0.43	70.7
Dashtestan2 (Dent-like)	0	-	12.7	41.5	42.3	45.4	2.04	11.7
	−0.2	-	13.1	40.0	43.3	45.1	1.51	15.9
	−0.4	-	11.1	35.0	40.0	45.0	0.82	29.6
	−0.6	-	11.0	29.5	35.0	44.0	0.65	36.6
	−0.8	-	12.4	23.6	25.0	40.8	0.19	117.1
Average	-	-	12.0	33.9	37.1	44.1	1.06	42.2
Oltan (Beta)	0	1.76	5.0	32.0	-	58.0	0.48	49.0
	−0.2	1.83	5.0	39.1	-	60.4	0.29	84.0
	−0.4	1.11	10.0	27.0	-	47.9	0.26	90.1
	−0.6	71.10	9.9	25.4	-	35.2	0.14	173.6
Average	-	-	7.5	30.9	-	50.4	0.29	99.1
Yellow-white (Beta)	0	17.37	5.0	49.0	-	65.0	0.34	72.5
	−0.2	4.90	10.0	35.0	-	53.2	1.44	16.7
	−0.4	8.51	10.0	38.1	-	53.2	0.72	33.3
	−0.6	3.60	10.0	32.9	-	44.3	0.19	123.9
	−0.8	241.8	3.2	23.6	-	46.8	0.07	331.1
Average	-	-	7.6	35.7	-	52.5	0.55	115.5
Naz (Segmented)	0	-	10.0	36.9	-	45.0	1.42	16.8
	−0.2	-	10.0	39.1	-	45.0	0.96	24.9
	−0.4	-	5.0	40.0	-	44.8	0.53	45.7
	−0.6	-	8.0	27.9	-	41.7	0.24	100.4
	−0.8	-	5.0	30.0	-	43.9	0.05	540.5
Average	-	-	7.6	34.8	-	44.1	0.65	145.7

Note: (a) the curvature of the beta model, T_b = base temperature (°C), T_o = optimum temperature (°C), T_{o1} = lower optimum temperature (°C), T_{o2} = upper optimum temperature (°C), and T_c = ceiling temperature (°C), Rmax = maximum germination rate, biological clock (h).

4. Discussion

The quantification of germination in ecological conditions regarding temperature and moisture can be very useful in determining germination rate and optimal seedling establishment. In other words, modeling science can evaluate the cardinal temperatures of plant seeds using seed germination models.

Our research revealed that drought stress caused by osmotic potential has reduced the germination rate in different sesame cultivars. Similar to the present research results, [26] for fenugreek (*Trigonella foenum-graecum* L.) seeds with deterioration and without deterioration showed that in conditions of reduced water availability, the biological clock of germination increased for sources. Drought stress and oxidative stress cause many gene damages, and by inhibiting the synthesis of gibberellin hormone, which plays a role in the activation of α-amylase, it causes a decrease in seed germination in moderate stresses and non-germination in severe pressures [27]. In another study by Ostadian Bidgoly et al. (2018) [12], in the quantification of the safflower seed germination response to temperature and different water potentials, they showed that the biological clock of germination

increased with the decrease in water potential, and the longest germination time at the optimal temperature was observed at a water potential of −1.6 MPa. By disrupting the process of water absorption by seeds, polyethylene glycol prevents the hydrolysis of stored materials and reduces the percentage and rate of germination [28]. The decrease in the seed germination rate can probably be attributed to the fact that the seeds need time to compensate for the damage caused to the membrane and other parts of the cell, restart the activity of the antioxidant system, and prevent oxidative stress. In another study on barley (*Hordeum vulgare* L.), it was also reported at a zero potential of 23.4 h that the water potential increased by 2.6 h/bar, which is probably due to the decrease in the rate of water absorption and the increase in the time of complete imbibition of the seeds to be able to germinate [29].

In many studies, the use of germination models to evaluate the reaction of plant seed germination to ecological conditions has been reported; therefore, in a study on safflower (*Carthamus tinctorius* L.) seedling emergence, the segmented model was chosen as the superior model. Cardinal temperatures, i.e., base, optimal, and ceiling temperatures, were determined as 3.4, 22, and 35 °C, respectively [30].

Soltani et al. (2014) [31] used a segmented model in their modeling studies of *Brassica napus* L. seed germination under the influence of temperature and water potential. According to their model, with a reduction in water potential, the base temperature gradually increased and reached about 6.7 °C at a water potential of −0.8 MPa. Using the beta model, [32] found that wild mustard (*Sinapis arvensis* L.) seeds cannot germinate at a base temperature lower than −2.9 °C. Moreover, the optimum germination temperature of wild mustard was about 22 °C under drought-stress conditions.

A more accurate evaluation to choose the best model among the three models presented with the priority of the correlation coefficient (rc) parameters due to checking the accuracy and precision of the model compared to other evaluation methods that only contain the model's accuracy. Moreover, root mean square error (*RMSE*), the coefficient explanation (R^2), the linear correlation coefficient (*r*), and coefficients *a* and *b*, respectively, indicate the distance of the regression line from the *X*-coordinates and the distance from the 1:1 line, which were selected for all six cultivars of sesame (Figure 4).

In the study on milk thistle (*Silybum marianum* L.), [33] showed that the beta model is the best model for predicting the time required to reach 50% germination and reported the cardinal temperatures (base temperature, optimal temperature, and ceiling temperature) as 5.19, 24.01, and 34.32 °C, respectively. In research by Nozari-Nejad et al. (2014) [34] quantifying the reaction of wheat (*Triticum aestivum* L.) germination to temperature and water potential, the dent-like model was reported as the superior model. Our research revealed that the dent-like model for Halil and Dashtestan2 cultivars, the beta model for Darab1 and Oltan cultivars, and the segmented model for Naz cultivars were selected as the superior models (Table 3). The cardinal temperatures were 1.5, 23.8, 33, and 41 °C for the base, sub-optimal, supra-optimal, and ceiling temperatures. In all cultivars in this research, with the increase in osmotic potential, the T_O, T_C, and Rmax had a decreasing trend, showing the dependence of this plant's T_O, T_C, and Rmax on water potential. At temperatures lower than the optimal temperature, there is a linear relationship between germination rate and temperature at all water potentials. Moreover, the optimum and ceiling temperatures were reported at zero water potential of 35.4 and 45.2 °C, respectively.

The lowest base potential in the velvetleaf (*Abutilon theophrasti* Medic.) plant was observed in the optimal temperature range, which is consistent with the present results, and with the increase in temperature after the optimum temperature, the value of the germination base potential increased linearly [35]. It can be concluded that the water potential is more effective in the germination process at temperatures higher than the optimum temperature. The osmotic potential is caused by polyethylene glycol by disrupting the process of water absorption by preventing the hydrolysis of seed-stored material and the internal activities of the seed, which causes a decrease in the germination rate [36].

Seed quality and composition are other factors affecting seed germination [10]. In oilseed plants, fatty acids play a significant role in seed germination and seedling establishment. In oilseeds, the lipid is the primary energy reservoir that provides essential energy for the developing embryo. Variations in seed oil affect membrane lipid composition in terms of function and membrane permeability, which affects germination, establishment, and tolerance to environmental stresses [37]. In oilseeds, the first step of food storage consumption is performed by the lipase enzyme, which breaks ester bonds and releases fatty acids and glycerol due to the activity of this enzyme [38,39].

The examination of nine sesame genotypes showed that the average base, optimum, and maximum temperatures in the assessed genotypes were 12.8, 38, and 49.3 °C, respectively [40]. In the present research, the average temperature in all water potentials of the base, sub-optimal, supra-optimum, and ceiling was determined as 12.6, 33.3, 38, and 43.9 °C, respectively. The highest base temperature (13.1 °C) and the lowest base temperature (7.5 °C) were obtained from Halil and Oltan cultivars, respectively. It can be stated that in terms of seed germination, the Halil cultivar with an increase in the ratio of saturated to unsaturated fatty acids is a cultivar sensitive to low-temperature stress, and the Oltan cultivar (decreased saturated/unsaturated) is considered a cold-resistant cultivar.

A significant amount of unsaturated fatty acids maintains membrane fluidity at low temperatures. There is more proof in favor of the hypothesis that raising polyunsaturated fatty acid concentrations can enhance seed performance at low temperatures [41]. When the seeds of oilseed plants are exposed to different temperatures, a wide range of cellular responses occur, including regulating fatty acid levels; in other words, in some seeds, lipid content is related to seed germination ability. In this regard, it has been reported that the power of tomato seeds to germinate at low temperatures is due to unsaturated fatty acids [42]. Additionally, during seed maturity, genotypes and their interactions with environmental factors, namely moisture and temperature, impact the synthesis of fatty acids and the proportion of oleic and linoleic acids in the seed [43].

The ambient temperature changes the ratio of linoleic acid during the growth of oilseeds. Depending on the geographical region and year, it leads to an unwanted change in the balance of oleic to linoleic in the final oil composition [44,45].

In this regard, lower temperatures (22 °C) have been reported to be associated with more linoleic acid synthesis due to increased oleate desaturase enzyme activity in peanut seed oil [46]. The present study showed that T_b had a negative linear correlation with the concentration of linoleic acid and a positive linear correlation with the concentration of oleic acid, which was in line with the results of Belo et al.'s 2014 research [20]. Possible mechanisms involved in these responses include changes in membrane function and the breakdown of storage lipids during germination. In this regard, a decrease in seed oil content was observed in safflower cultivars under drier conditions. It may be attributed to a reduction in the availability of carbohydrates for oil synthesis [47].

5. Conclusions

A change in the environmental factors affecting the quality of sesame seed fatty acids will affect the ability of the source to germinate. This research showed that six cultivars of the same species can show optimal temperatures and other reactions to environmental conditions so that the germination rates of Halil and Dashtestan2 cultivars follow the dent-like model. Moreover, Darab1, Oltan, and Yellow-White cultivars follow the beta model, and Naz cultivars follow the segmented model. Accordingly, the average of the base temperature (12.6 °C), the sub-optimal (33.3 °C), the supra-optimal (38 °C), and the ceiling (43.9 °C) were for the dent-like model. The average temperatures of the base, optimal, and top were determined for the numbers 8.5, 31.5, and 50.5 °C, respectively, with the beta model. According to the result, the Halil cultivar with higher oleic, palmitic, and arachidic acids has higher base temperatures suitable for later planting dates. Moreover, the results of this investigation suggest that the Naz cultivar that takes a long time to germinate has a long biological clock for early cultivation, and the Dashtestan2 cultivar

with high germination rates is suitable for cultivation in areas where water stress and high-temperature stress occur. Considering that this research was conducted only on six cultivars of sesame and its results are limited, it is suggested that significantly more work should be conducted to determine the role of seed compounds on the germination of many sesame cultivars under different conditions.

Author Contributions: H.B.: Conceptualization; research supervision; formal analysis; methodology; data curation. V.S.K.: Performed the experimental work and wrote the first draft as part of the M.Sc. project. S.Z.H.: Data and figure editing. A.M. and M.G.: Supervision and M.Sc. project administration. R.P.: Manuscript improvement and editing. B.D.: Final manuscript review and editing. All authors have read and agreed to the published version of the manuscript.

Institutional Review Board Statement: Not applicable.

Data Availability Statement: The data presented in this study are available on request from the corresponding author. The data are not publicly available due to Yasouj University rules.

Conflicts of Interest: The authors declare no conflict of interest.

References

1. Kozłowska, W.; Matkowski, A.; Zielińska, S. Light intensity and temperature effect on *Salvia yangii* (BT Drew) metabolic profile in vitro. *Front. Plant Sci.* **2022**, *13*, 888509. [CrossRef] [PubMed]
2. Donohue, K.; Casas, R.R.D.; Burghardt, L.; Kovach, K.; Willis, C.G. Germination, post-germination adaptation, and species ecological ranges. *Annu. Rev. Ecol. Syst.* **2010**, *41*, 293–319. [CrossRef]
3. Savaedi, Z.; Parmoon, G.; Moosavi, S.A.; Bakhshande, A. Light and Gibberellic Acid's role in cardinal temperatures and thermal time required for the Charnushka (*Nigella sativa*) seed germination. *Ind. Crops Prod.* **2019**, *132*, 140–149. [CrossRef]
4. Sanehkoori, F.H.; Pirdashti, H.; Bakhshandeh, E. Quantifying water stress and temperature effects on camelina (*Camelina sativa* L.) seed germination. *Environ. Exp. Bot.* **2021**, *186*, 104450. [CrossRef]
5. Saeed, S.; Ullah, A.; Ullah, S.; Noor, J.; Ali, B.; Khan, M.N.; Hashem, M.; Mostafa, Y.S.; Alamri, S. Validating the impact of water potential and temperature on seed germination of wheat (*Triticum aestivum* L.) via hydrothermal time model. *Life* **2022**, *12*, 983. [CrossRef] [PubMed]
6. Sghaier, H.; Tarnawa, A.; Khaeim, H.; Kovács, G.P.; Gyuricza, C.; Kende, Z. The effects of temperature and water on rapeseed seed germination and seedling development (*Brassica napus* L.). *Plants* **2022**, *11*, 2819. [CrossRef] [PubMed]
7. Zhang, R.; Chen, D.; Liu, H.; Guo, C.; Tang, L.; Wang, H.; Chen, Y.; Luo, K. Effect of temperature and water potential on the germination of seeds from three different populations of *Bidens pilosa* as a potential Cd hyperaccumulator. *BMC Plant Biol.* **2022**, *22*, 487. [CrossRef]
8. Khan, W.; Shah, S.; Ullah, A.; Ullah, S.; Amin, F.; Iqbal, B.; Ahmad, N.; Abdel-Maksoud, M.A.; El-Zaidy, M.; Al-Qahtani, W.H.; et al. Utilizing hydrothermal time models to assess the effects of temperature and osmotic stress on maize (*Zea mays* L.) germination and physiological responses. *BMC Plant Biol.* **2023**, *23*, 414. [CrossRef]
9. Wang, H.; Zhao, K.; Li, X.; Chen, X.; Liu, W.; Wang, J. Factors affecting seed germination and emergence of *Aegilops tauschii*. *Weed Res.* **2020**, *60*, 171–181. [CrossRef]
10. Bewley, J.; Bradford, K.; Hilhorst, H.; Nonogaki, H. *Seeds: Physiology of Development, Germination, and Dormancy*, 3rd ed.; Springer: Cham, Switzerland, 2013; pp. 85–246.
11. Bello, P.; Bradford, K.J. Relationships of Brassica seed physical characteristics with germination performance and plant blindness. *Agriculture* **2021**, *11*, 220. [CrossRef]
12. Ostadian Bidgoly, R.; Balouchi, H.; Soltani, E.; Moradi, A. Effect of temperature and water potential on *Carthamus tinctorius* L. Seed germination: Quantification of the cardinal temperature and modeling using hydrothermal time. *Ind. Crops Prod.* **2018**, *113*, 121–127. [CrossRef]
13. Rowse, H.R.; Finch-Savage, W.E. Hydrothermal threshold models can describe the germination response of carrot (*Daucus carota*) and onion (*Allium cepa*) seed populations across both sub-and supra-optimal temperatures. *New Phytol.* **2003**, *158*, 101–108. [CrossRef]
14. UCana, K.; Killi, F. Effects of different irrigation programs on flower and capsule numbers and shedding percentage of sesame. *Agric. Water Manag.* **2010**, *98*, 227–233. [CrossRef]
15. Rostami, M.; Farzaneh, V.; Boujmehrani, A.; Mohammadi, M.; Bakhshabadi, H. Optimizing the extraction process of sesame seedś oil using response surface method on the industrial scale. *Ind. Crops Prod.* **2014**, *58*, 160–165. [CrossRef]

16. Were, B.A.; Onkware, A.O.; Gudu, S.; Welander, M.; Carlsson, A.S. Seed oil content and fatty acid composition in East African sesame (*Sesamum indicum* L.) accessions evaluated over three years. *Field Crops Res.* **2006**, *97*, 254–260. [CrossRef]

17. Ahmed, I.A.M.; AlJuhaimi, F.; Özcan, M.M.; Ghafoor, K.; Şenay Şimşek, S.; Babiker, E.E.; Osman, M.A.; Gassem, M.A.; Salih, H.A.A. Evaluation of chemical properties, amino acid contents, and fatty acid compositions of sesame seed provided from different locations. *J. Oleo Sci.* **2020**, *69*, 795–800. [CrossRef]

18. Dossa, K.; Li, D.; Zhou, R.; Yu, J.; Wang, L.; Zhang, Y.; Zhang, X. The genetic basis of drought tolerance in the high oil crop *Sesamum indicum*. *Plant Biotechnol. J.* **2019**, *17*, 1788–1803. [CrossRef]

19. Langyan, S.; Yadava, P.; Sharma, S.; Gupta, N.C.; Bansal, R.; Yadav, R.; Kalia, S.; Kumar, A. Food and nutraceutical functions of sesame oil: An underutilized crop for nutritional and health benefits. *Food Chem.* **2022**, *389*, 132990. [CrossRef]

20. Belo, R.G.; Tognetti, J.; Benech-Arnold, R.; Izquierdo, N.G. Sunflowers' seed oil composition affects germination responses to temperature and water potential. *Ind. Crops Prod.* **2014**, *62*, 537–544. [CrossRef]

21. Michel, B.E.; Kaufmann, M.R. The osmotic potential of polyethylene glycol 6000. *Plant Physiol.* **1973**, *51*, 914–916. [CrossRef]

22. Soltani, A.; Robertson, M.; Torabi, B.; Yousefi-Daz, M.; Sarparast, R. Modeling seedling emergence in chickpeas as influenced by temperature and sowing depth. *Agric. For. Meteorol.* **2006**, *138*, 156–167. [CrossRef]

23. Yol, E.; Toker, R.; Golukcu, M.; Uzun, B. Oil content and fatty acid characteristics in Mediterranean sesame core collection. *Crop Sci.* **2015**, *55*, 2177–2185. [CrossRef]

24. Azadmard-Damirchi, S.; Habibi-Nodeh, F.; Hesari, J.; Nemati, M.; Fathi Achachlouei, B. Effect of pretreatment with microwaves on oxidative stability and nutraceuticals content of oil from rapeseed. *Food Chem.* **2010**, *121*, 1211–1215. [CrossRef]

25. Azadmard-Damirchi, S.; Dutta, P.C. A novel solid-phase extraction method separates 4-desmethyl-, 4-monomethyl-, and 4, 4′-dimethyl sterols in vegetable oils. *J. Chromatogr. A* **2006**, *1108*, 183–187. [CrossRef] [PubMed]

26. Teimori, H.; Balouchi, H.; Moradi, A.; Soltani, E. Effect of seed aging and water potential on seed germination and biochemical indices of Fenugreek (*Trigonella foenum-graecum*) at different temperatures. *Iran. J. Seed Res.* **2019**, *5*, 105–128. [CrossRef]

27. Tajlil, A.H.; Pazoki, A.; Eradatmand Asli, D. Effects of seed priming by mannitol and zinc sulfate on biochemical parameters and seed germination of chickpea. *Int. J. Farming Allied Sci.* **2014**, *3*, 294–298.

28. Hoseini, A.; Salehi, A.; Sayyed, R.Z.; Balouchi, H.; Moradi, A.; Piri, R.; Fazeli-Nasab, B.; Poczai, P.; Ansari, M.J.; Obaid, S.A.; et al. Efficacy of biological agents and fillers seed coating in improving drought stress in anise. *Front. Plant Sci.* **2022**, *13*, 955512. [CrossRef]

29. Khalili, N.; Soltani, A.; Zeinali, E.; Ghaderi far, F. Evaluation of nonlinear regression models to quantify barley germination rate response to temperature and water potential. *J. Crop Prod.* **2015**, *7*, 40–23.

30. Torabi, B.; Soltani, E.; Archontoulis, S.V.; Rabii, A. Temperature and water potential effects on *Carthamus tinctorius* L. Seed germination: Measurements and modeling using hydrothermal and multiplicative approaches. *Braz. J. Bot.* **2016**, *39*, 427–436. [CrossRef]

31. Soltani, E.; Oveisi, M.; Soltani, A.; Galeshi, S.; Ghaderifar, F.; Zeinali, E. Affected by temperature and water Seed germination modeling of volunteer canola as potential: Hydrothermal time model. *Weed Res. J.* **2014**, *6*, 23–38.

32. Soltani, E.; Soltani, A.; Galeshi, S.; Ghaderi-Far, F.; Zeinali, E. Seed germination modeling of wild mustard (*Sinapis arvensis* L.) as affected by temperature and water potential: Hydrothermal time model. *J. Plant Prod. Res.* **2013**, *20*, 19–34.

33. Parmoon, G.; Moosavi, A.; Akbari, H.; Ebadi, A. Quantifying cardinal temperatures and thermal time required for germination of *Silybum marianum* seed. *Crop J.* **2015**, *3*, 145–151. [CrossRef]

34. Nozari-Nejad, M.; Zeinali, E.; Soltani, A.; Soltani, E.; Kamkar, B. Quantify wheat germination rate response to temperature and water potential. *J. Crop Prod.* **2014**, *6*, 117–135.

35. Yasari, E.; Miri, M.; Atashi, S.; Jamali, M. Application of hydrothermal time model to determine the cardinal temperatures for seed germination in crops (A case study; velvetleaf (*Abutilon theophrasti* Med.)). *Iran. J. Seed Sci. Technol.* **2018**, *7*, 85–94.

36. Queiroz, M.S.; Oliveira, E.S.; Steiner, F.; Zuffo, A.M.; Zoz, T.; Vendruscolo, E.P.; Silva, M.V.; Mello, F.F.R.; Cabral, R.C.; Menis, F.T. Drought stresses seed germination and early growth of maize and sorghum. *J. Agric. Sci.* **2019**, *11*, 310–318. [CrossRef]

37. Sun, M.; Spears, J.F.; Isleib, T.G.; Jordan, D.L.; Penny, B.; Johnson, D.; Copeland, S. Effect of production environment on seed quality of normal and high-oleate large seeded Virginia-type peanut (*Arachis hypogaea* L.). *Peanut Sci.* **2014**, *41*, 90–99. [CrossRef]

38. Moosavi, S.A.; Siadat, S.A.; Poshtdar, A.; Direkvand, F. Ultrasonic-assisted seed priming to alleviate aging damages to milk thistle (*Silybum marianum*) seeds. *Not. Sci. Biol.* **2018**, *10*, 275–281. [CrossRef]

39. Asadi Aghbolaghi, M.; Sedghi, M.; Sharifi, R.S.; Dedicova, B. Germination and the biochemical response of pumpkin seeds to different concentrations of humic acid under cadmium stress. *Agriculture* **2022**, *12*, 374. [CrossRef]

40. Ghadri-Far, F.; Soltani, E. Evaluation of sesame cultivars germination on response to temperature: Determination of cardinal temperatures and thermal tolerance. *Iran. J. Field Crop Sci.* **2015**, *46*, 473–483. [CrossRef]

41. Oteng, A.; Kersten, S. Mechanisms of action of trans fatty acids. *Adv. Nutr.* **2020**, *11*, 697–708. [CrossRef]

42. Islam, S.; Carmen, R.C.; Garner, J.O. Fatty acid compositions in ungerminated (whole seed), cotyledon, and embryo tissues of cowpea (*Vigna unguiculata* L. Walp) seed grown under different temperatures. *J. Food Agric. Environ.* **2007**, *5*, 190–196.

43. Yeilaghi, H.; Arzani, A.; Ghaderian, M.; Fotovat, R.; Feizi, M.; Pourdad, S.S. Effect of salinity on seed oil content and fatty acid composition of safflower (*Carthamus tinctorius* L.) genotypes. *Food Chem.* **2012**, *130*, 618–625. [CrossRef]

44. Martinez-Rivas, L.M.; Gracia-Diaz, M.T.; Mancha, M. Temperature and oxygen regulation of microsomal oleate desaturase (FAD2) from sunflower. *Biochem. Soc.* **2000**, *28*, 890–892. [CrossRef]

45. Rabiei, Z.; Tahmasebi, E.S.; Vannozzi, G.P. Regulation of polyunsaturated fatty acids accumulation and characterization of linolenic acid after sunflower seed germination. *Helia* **2007**, *30*, 175–182. [CrossRef]
46. Sogut, T.; Ozturk, F.; Kizil, S. Effect of sowing time on peanut (*Arachis hypogaea* L.) cultivars: I.e.; yield, yield components, oil, and protein content. *Sci. Pap. Ser. A Agron.* **2016**, *59*, 415–420. [CrossRef]
47. Sehgal, A.; Sita, K.; Siddique, K.H.M.; Kumar, R.; Bhogireddy, S.; Varshney, R.K.; HanumanthaRao, B.; Nair, R.M.; Prasad, P.V.V.; Nayyar, H. Drought and Heat-Stress Effects on Seed Filling in Food Crops: Impacts on Functional Biochemistry, Seed Yields, and Nutritional Quality. *Front. Plant Sci.* **2018**, *9*, 1705. [CrossRef]